



# Global transcriptomic analysis in avocado nursery trees reveals differential gene expression during asymptomatic infection by avocado sunblotch viroid (ASBVd)

M. Joubert<sup>a,b</sup>, N. van den Berg<sup>a,b</sup>, J. Theron<sup>a</sup>, V. Swart<sup>a,b,\*</sup>

<sup>a</sup> Department of Biochemistry, Genetics and Microbiology, Faculty of Natural and Agricultural Sciences, University of Pretoria, Pretoria, Gauteng, South Africa

<sup>b</sup> Hans Merensky Chair in Avocado Research, Forestry and Agricultural Biotechnology Institute, University of Pretoria, Pretoria, Gauteng, South Africa

## ARTICLE INFO

### Keywords:

Avocado sunblotch  
*Persea americana*  
ASBVd  
RNA-seq  
Avocado transcriptome  
Viroid infection

## ABSTRACT

Avocado sunblotch viroid (ASBVd) is the type species of the family *Avsunviroidae* and the causal agent of avocado sunblotch disease. The disease is characterised by the presence of chlorotic lesions on avocado fruit, leaves and/or stems. Infected trees may remain without chlorosis for extended periods of time, though distorted growth and reduced yield has been observed in these cases. The molecular effects of ASBVd on avocado, and members of the *Avsunviroidae* on their respective hosts in general, remain poorly understood. Host global transcriptomic studies within the family *Pospiviroidae* have identified several host pathways that are affected during these plant-pathogen interactions. In this study, we used RNA sequencing to investigate host gene expression in asymptomatic avocado nursery trees infected with ASBVd. Transcriptome data showed that 631 genes were differentially expressed, 63 % of which were upregulated during infection. Plant defence responses, phytohormone networks, gene expression pathways, secondary metabolism, cellular transport as well as protein modification and degradation were all significantly affected by ASBVd infection. This work represents the first global gene expression study of ASBVd-infected avocado, and the transcriptional reprogramming observed during this asymptomatic infection improves our understanding of the molecular interactions underlying broader avsunviroid-host interactions.

## 1. Introduction

Avocado sunblotch viroid (ASBVd) is a circular, single-stranded RNA molecule of approximately 250 nucleotides, and is the causal agent of avocado sunblotch disease (Allen et al., 1981; Palukaitis et al., 1979; Symons, 1981). The disease is distinguished by the presence of chlorotic symptoms on avocado (*Persea americana* Mill.), which include the formation of white, yellow, or red sunken lesions on avocado fruit, discoloured streaks on young stems, and discolouration and malformation of leaves. While the appearance of chlorotic lesions is characteristic of the disease, the viroid may also infect avocado without causing notable chlorosis. These “asymptomatic” (chlorosis-free) infections are common in avocado orchards and nurseries, and are associated with decreased yield of mature trees, leading to economic implications for growers (Kuhn et al., 2017). Previous studies have linked asymptomatic and symptomatic leaf infections to the presence of specific viroid variants (Schnell et al., 2001a, 2001b; Semancik and Szychowski, 1994), though

the exact mutation within the ASBVd genome responsible for chlorosis remains unknown.

ASBVd is the exemplar member of the family *Avsunviroidae* — a small viroid family of five known species, which all localise to plastids in host cells. Avsunviroids can be distinguished by their symmetrical rolling circle mechanism of replication in host plastids, and their ability to form hammerhead ribozymes, which enable self-cleavage (Di Serio et al., 2018). These viroids cause disease symptoms which were described by Flores et al. (2020) as “specific and local”. Variants of peach latent mosaic viroid (PLMVd), for example, cause peach yellow mosaic disease and peach calico, while chrysanthemum chlorotic mottle viroid (CChMVd) causes chrysanthemum chlorotic mottle disease (Flores et al., 2017a, 2017b). These diseases, like avocado sunblotch, are characterised by chlorotic symptoms that form only on localised parts of infected hosts such as leaves, fruit, flowers, and/or stems. Previous studies on PLMVd have linked the particular symptoms caused by different variants to specific mutations within the viroid genome

\* Corresponding author.

E-mail address: [velushka.swart@fab.up.ac.za](mailto:velushka.swart@fab.up.ac.za) (V. Swart).

<https://doi.org/10.1016/j.virusres.2023.199263>

Received 23 August 2023; Received in revised form 1 November 2023; Accepted 6 November 2023

Available online 10 November 2023

0168-1702/© 2023 The Author(s). Published by Elsevier B.V. This is an open access article under the CC BY-NC-ND license (<http://creativecommons.org/licenses/by-nc-nd/4.0/>).

(Delgado et al., 2019; Navarro et al., 2012). Similarly, mutations to a specific region of the CChMVd genome have been linked to chlorotic symptoms (Serra et al., 2023), providing further evidence as to the role of RNA silencing in pathogenesis of members of the family *Avsunviroidae* (Flores et al., 2020).

The second viroid family is the family *Pospiviroidae* (type species *Potato Spindle Tuber Viroid* (PSTVd)) and includes at least 39 known species. Members of this family use an asymmetrical rolling circle method to replicate in host nuclei and contain a central conserved region (CCR) within their genomes (Di Serio et al., 2021). Pospiviroids cause diseases that are fundamentally different from those caused by avsunviroids, in that the symptoms they trigger are “non-specific and systemic” (Flores et al., 2020). Stunting, for example, is a symptom induced by several pospiviroids (such as hop stunt viroid (HSVd), citrus dwarfing viroid (CDVd) and chrysanthemum stunt viroid (CSVd)), and this systemic symptom cannot be directly linked to silencing of specific RNAs due to simple pospiviroid genome mutations, unlike what has been shown for avsunviroids (Flores et al., 2020).

While the molecular mechanisms underlying pospiviroid pathogenesis are still being explored, there has been significant progress made in understanding how diseased hosts respond to infection by members of the *Pospiviroidae* family; largely due to investigations into differential gene expression in affected hosts (reviewed by Joubert et al. (2022)). In recent years, next-generation sequencing (NGS) technology has enabled the global transcriptomic analyses of several different hosts infected with PSTVd (Chi et al., 2022; Góra-Sochacka et al., 2019; Hadjieva et al., 2021; Więsyk et al., 2020), HSVd (Xia et al., 2017; Xu et al., 2020), citrus exocortis viroid (CEVd) (Wang et al., 2019), CDVd (Lavagi-Craddock et al., 2022) and dendrobium viroid (DVd) (Li et al., 2022). These studies have shown that several host pathways were commonly altered by pospiviroid infection, including host defence signalling, phytohormone networks, secondary metabolism, transport, transcription, as well as protein synthesis and modification (Joubert et al., 2022).

In contrast, transcriptome data generated to date for avsunviroid-infected plants is limited, and so the effect of avsunviroids on their hosts remains poorly understood. A microarray analysis revealed that asymptomatic peach infected with peach latent mosaic viroid (PLMVd) had less than 20 genes with altered expression (Herranz et al., 2013). The effect of ASBVd infection on the avocado transcriptome has thus far only been studied on a small scale, using reverse transcriptase quantitative PCR (RT-qPCR). Gene expression changes of four avocado genes in infected leaves and fruit showed that two genes encoding pathogenesis-related (PR) proteins were induced upon ASBVd infection of fruits (López-Rivera et al., 2018). The expression of *ethylene responsive element binding protein* (*EREBP*) and *Nonexpressor of pathogenesis-related 1* (*NPR1*) was, however, not significantly altered. Despite the limited expression changes investigated by López-Rivera et al. (2018), that study is the only investigation into the transcriptome of ASBVd-infected avocado to date, and therefore represented a starting point for further exploration into host defence initiation upon ASBVd infection.

To elucidate the effects of ASBVd on avocado, we used RNA sequencing (RNA-seq) to produce a global transcriptome for asymptomatic nursery trees which were infected with the viroid. Expression analysis revealed that over 600 genes were differentially expressed during infection, especially those involved in host defence, transcription, and protein modification and degradation. Our results reveal novel insights into the impact of ASBVd on global gene expression in avocado, which contributes substantially to the current understanding of diseases caused by members of the *Avsunviroidae* family.

## 2. Materials and methods

### 2.1. Plant material and RNA extraction

Two-year-old avocado trees, produced from seedlings grafted with Hass budwood obtained from an orchard with ASBVd-infected trees,

were provided by a nursery in KwaZulu-Natal, South Africa, to the University of Pretoria. The 44 nursery trees were kept in a climate-controlled phytotron (25 °C, 70 % relative humidity) with a 16 h/8 h day/night photoperiod while infection status was confirmed.

For the isolation of RNA, the first fully emerged leaves from branch tips were harvested from nursery trees without visible sunblotch symptoms. Six leaves were harvested from representative branches of each tree (representing one biological replicate) and pooled to form one sample. Pooled leaves were flash frozen in liquid nitrogen and ground to a fine powder using an IKA® Tube Mill (IKA®, Staufen, Germany). Ground leaf material was stored at −70 °C before RNA was extracted from 2 g of the pooled material for each sample. RNA was isolated using a modified CTAB RNA extraction method (Chang et al., 1993). Extracted RNA was treated with DNase I (New England Biolabs® Inc., Ipswich, Massachusetts, USA) before purification using the RNeasy® MinElute® Cleanup Kit (Qiagen, Valencia, California, USA). The quality and concentration of purified RNA was determined using a NanoDrop™ 2000 spectrophotometer (Thermo Fisher Scientific, Waltham, Massachusetts, USA) and confirmed by electrophoresis on a 2 % agarose gel.

### 2.2. ASBVd detection

Infection status of the 44 Hass-grafted seedlings (without chlorotic symptoms) was confirmed using a protocol modified from Kuhn et al. (2019). RNA extracted from each sample was reverse transcribed to ASBVd cDNA using the High-Capacity cDNA Archive Kit from Applied Biosystems™ (Thermo Fisher Scientific) following manufacturer's instructions, modified using ASBVd-specific SB1-F1 and SB1-R1 primers (Table S1). Viroid cDNA was pre-amplified by PCR using the same primers and FastStart™ Taq DNA Polymerase from Roche Applied Science (Merck KGaA, Darmstadt, Germany). Pre-amplification reactions contained 1 U polymerase enzyme, 1X PCR Reaction Buffer, 2 mM MgCl<sub>2</sub>, 200 μM of each dNTP, 0.2 μM of each primer, respectively, 2 μl cDNA template and sterile water to a total volume of 25 μl. Reactions were incubated in a Veriti™ 96-Well Fast Thermal Cycler from Applied Biosystems™ (Thermo Fisher Scientific) under the following cycling conditions: 94 °C for 4 min, 15 cycles of 30 s at 94 °C, 30 s at 60 °C and 30 s at 72 °C, followed by 7 min at 72 °C.

Nested real-time PCR was carried out using TaqMan™ Gene Expression Master Mix from Applied Biosystems™ (Thermo Fisher Scientific) with the internal viroid primers ASBVd2qPCR-F and ASBVd2qPCR-R designed by Morey-León et al. (2018) and the ASBTM probe modified from Geering et al. (2006) (Table S1). Reactions were carried out in triplicate for each sample in a 96-well plate, with each reaction containing 2 μl template (pre-amplification product), 1X TaqMan™ Gene Expression Master Mix, 0.4 μM of each primer, 0.2 μM probe, and sterile water to a total volume of 20 μl. Amplification was carried out in a CFX Connect™ Real-Time PCR System (Bio-Rad Laboratories, Hercules, California, USA) and thermocycling conditions were: 50 °C for 2 min, 95 °C for 10 min, followed by 40 cycles of 15 s at 95 °C, and 1 min at 60 °C. Each detection plate contained a non-template control (NTC), the NTCs from respective cDNA synthesis and pre-amplification reactions, an uninfected control, and a known infected sample (from symptomatic leaf material). Presence of ASBVd was detected by fluorescence during real-time PCR compared to uninfected controls, while absence of the viroid was confirmed by lack of fluorescence.

Following initial screening of 44 nursery trees, the 24 trees most similar in size and condition were selected for a second round of detection screening. This second detection assay served to confirm the results from the initial screening by including additional controls throughout the assay. This was accomplished using RNA extracted from freshly harvested leaves (as before), with leaves from a symptomatic infected tree and a known uninfected tree being used as controls during harvesting and RNA extraction, in addition to the detection assay NTCs mentioned previously.

### 2.3. Transcriptome sequencing

Following the confirmation of infection status of 24 Hass-grafted seedlings, six infected and six uninfected trees were selected for RNA-seq. Leaves were harvested and RNA was extracted as before. An aliquot of this RNA was used for a final confirmation of the presence or absence of the viroid by real-time PCR, and amplified products were electrophoresed on a 2 % agarose gel to confirm that fluorescence corresponded with amplification of the desired product. The remaining purified total RNA was sent to Macrogen (Macrogen Europe, Amsterdam, The Netherlands) for sequencing. Integrity of RNA was determined using an Agilent 2100 Bioanalyzer (Agilent Technologies, Santa Clara, California, USA). Sequencing libraries were constructed by Macrogen using the TruSeq Stranded mRNA Library Prep kit (Illumina, San Diego, California, USA), and prepared libraries were used for paired-end sequencing on an Illumina Novaseq 6000 platform (PE150). Raw NGS data were deposited in the Sequence Read Archive of NCBI GenBank (accession number PRJNA1001370).

### 2.4. Sequencing of ASBVd in infected samples

Sanger sequencing was used as an additional confirmation of the presence of ASBVd in all infected samples. Briefly, ASBVd cDNA generated for detection purposes was amplified by PCR using Phusion Hot Start II High-Fidelity DNA Polymerase (Thermo Fisher Scientific) in a 20 µl reaction containing 1X Phusion HF buffer, 200 µM of each dNTP, 0.2 U Phusion polymerase, 2 µl cDNA template and 0.5 µM of each primer, SB1-F1 and SB1-R1 (Table S1), respectively. Reactions were incubated in a Veriti™ 96-Well Fast Thermal Cycler, with the following cycling conditions: 98 °C for 1 min, 30 cycles of 10 s at 98 °C, 30 s at 60 °C and 10 s at 72 °C, followed by 5 min at 72 °C. PCR products were visualised on a 1 % agarose gel and purified using the Zymoclean™ Gel DNA Recovery Kit (Zymo Research, Irvine, California, USA).

Purified PCR products were quantified using a NanoDrop™ 2000 spectrophotometer (Thermo Fisher Scientific) and cloned into *Escherichia coli* DH5α using the Invitrogen Zero Blunt™ TOPO™ PCR Cloning Kit (Thermo Fisher Scientific) according to manufacturer's guidelines. Plasmids were extracted using the QIAprep® Spin Miniprep Kit (Qia-gen). For each infected sample, five plasmids were sequenced in both directions using M13-F (5'-GTAAACGACGACGCGCCAGT-3') and M13-R (5'-CAGGAAACAGCTATGAC-3') primers. Sequencing reactions were set up in a volume of 12 µl made up of the following reagents: 0.85X sequencing buffer, 4.17 % v/v BigDye 3.1, 0.83 µM primer and 40–200 ng plasmid DNA. The sequencing PCR was performed in a Veriti™ 96-Well Fast Thermal Cycler set at 96 °C for 5 s, followed by 25 cycles of 10 s at 96 °C, 5 s at 55 °C and 4 min at 60 °C. Products of sequencing reactions were purified using a sodium acetate precipitation before they were submitted to the DNA Sanger sequencing facility at the University of Pretoria (Faculty of Natural and Agricultural Sciences) for sequencing using an ABI 3500xl genetic analyser (Applied Biosystems, Thermo Fisher Scientific). Obtained sequences were analysed and assembled in CLC Main Workbench v21.0.1. to produce sequencing contigs for each individual clone and were then aligned to the ASBVd type sequence SB-1 (Symons, 1981) using default parameters to confirm sequence identity. The seven unique sequences amongst the 30 clones were uploaded as separate variants to NCBI GenBank under accession numbers OR359952-OR359958.

### 2.5. Differential gene expression analysis

Raw Illumina RNA-seq reads were processed using Trimmomatic v0.39 (Bolger et al., 2014) to remove sequencing adaptors, and to filter out low quality reads and those shorter than 36 bp. The quality of filtered RNA-seq data was assessed using FastQC v0.11.9 (Andrews, 2010) and summarised using MultiQC v1.13a (Ewels et al., 2016). Filtered reads were aligned to the *P. americana* West Indian (WI) pure

accession genome (Peame105) (Avocado Genome Consortium, personal communication) using HISAT2 v2.2.1 (Kim et al., 2015). Aligned reads were processed using samtools v1.6 (Li et al., 2009) and quantified using featureCounts (Liao et al., 2014).

The counts matrix obtained from featureCounts was imported into RStudio v2022.12.0.353 (Posit Team, 2022), and DESeq2 v1.38.3 (Love et al., 2014) was used to analyse the count data. Differential gene expression analysis was performed using the Wald test, with the uninfected samples as a reference. The Benjamini and Hochberg approach was used to adjust *p*-values by accounting for false discovery rate. Genes with an adjusted *p*-value (*padj*) < 0.05 were considered as significantly differentially expressed genes (DEGs). The normalised DEGs determined by DESeq2 were then transformed using the 'varianceStabilizing-Transformation' (VST) function, and 'plotPCA' was used to visualise the principal component analyses (PCA) of the transformed data.

### 2.6. Functional classification of differentially expressed genes

To categorise DEGs according to their functions, Gene Ontology (GO) enrichment analysis was carried out using the GOSec package in RStudio (Young et al., 2010). Over-represented GO terms amongst up- or downregulated DEGs, with log<sub>2</sub>FoldChange (log<sub>2</sub>FC) ≥ 0.58 or ≤ −0.58 (fold change 1.5X higher or lower), respectively, were considered significantly enriched at *p* < 0.05.

MapMan v3.6.0RC1 (Schwacke et al., 2019) was used for further functional classification of DEGs (with the same log<sub>2</sub>FC threshold). MapMan bins were previously assigned for avocado proteins from the genome by Backer et al. (2022), using Mercator v3.6 (Lohse et al., 2014). Those bins were used to link DEGs from this experiment to specific host pathways. For particular pathways of interest, heatmaps were generated using the pheatmap package in RStudio (Kolde, 2012) for visualisation.

### 2.7. RT-qPCR validation of differentially expressed genes

RT-qPCR analysis was used to validate the RNA-seq data. Aliquots containing 1 µg of the purified avocado RNA samples sent for Illumina sequencing were reverse transcribed to cDNA using the ImProm-II™ Reverse Transcription System (Promega Corporation, Madison, Wisconsin, USA) according to manufacturer's instructions, using oligo(dT) primers. Successful cDNA synthesis and absence of genomic DNA contamination was confirmed using the intron-spanning F3H primers (Table S1) in a FastStart™ Taq PCR with the same conditions as Engelbrecht et al. (2013).

Primers were designed for nine candidate genes (Table S1) using the online PrimerQuest™ Tool (Integrated DNA Technologies, Inc., <https://eu.idtdna.com/pages/tools/primerquest>). The primer efficiency was assessed by generating standard curves for the nine DEGs as well as two reference genes (*GAPDH* and *Polyubiquitin*), using serial dilutions of cDNA pooled from all biological replicates (1:5, 1:10, 1:50, 1:100, 1:250, 1:500, 1:1000).

RT-qPCR reactions were set up in 96-well plates using the KAPA SYBR® FAST qPCR Master Mix (2X) Kit (Sigma-Aldrich, Missouri, USA) according to manufacturer's instructions. Thermal cycling was carried out in a CFX Connect™ Real-Time PCR System as follows: 95 °C for 5 min, 40 cycles of 95 °C for 5 s, 58 °C for 20 s and 72 °C for 5 s, followed by 60 to 95 °C at 0.5 °C increments for 5 s to generate dissociation curves. Quantification of target genes was determined by normalising fluorescence data against the reference genes. Fold change of DEGs in infected samples was calculated using the ΔΔC<sub>q</sub> method in Bio-Rad CFX Maestro Software v2.2 (Bio-Rad Laboratories) and statistical significance was determined by a one-way ANOVA and Tukey test. Genes were considered significantly differentially expressed in infected samples relative to uninfected samples at *p* < 0.05.

### 3. Results

#### 3.1. ASBVd detection in asymptomatic nursery trees

To obtain ASBVd-infected and uninfected material for NGS, multiple rounds of screening were carried out to confirm presence or absence of the viroid. Following initial screening, ASBVd was detected in 17 of the 44 samples. A second detection assay, performed on newly harvested leaves from 24 trees (14 suspected to be infected), confirmed the presence of ASBVd in eight samples. Twelve trees were subjected to a third round of screening to validate results of the second detection assay prior to Illumina sequencing (Table S2). Real-time PCR produced fluorescence in the six infected samples (ASBVd 1–6 (A1–6)) (Figure S1a) but not in the six uninfected samples (Control 1–6 (C1–6)) (Figure S1b). Gel electrophoresis of PCR products (Figure S1c) showed that the ~155 bp region of the viroid was amplified in the positive control (P, known infected sample) and in the six infected replicates (A1–6), while no amplification was observed in the non-template control (N) or the six uninfected replicates (C1–6).

Viroid reads could not be detected in NGS data, since library preparation for mRNA sequencing used oligo-dT beads to capture poly-A tails. Sanger sequencing was therefore used to confirm the occurrence of ASBVd in the six infected samples. Five clones produced from each infected sample were all successfully aligned to ASBVd type sequence SB-1 (Symons, 1981) with only minor nucleotide differences (Figure S2). These small sequence changes are indicative of different ASBVd variants present in infected samples, confirming that viroid populations formed quasi-species in the tested nursery trees, as previously reported in mature avocado by Schnell et al. (2001a).

#### 3.2. Next-generation sequencing and differential gene expression analysis

Illumina sequencing of RNA extracted from six infected and six

uninfected samples produced 43.7–53.1 million raw paired-end reads per sample, of which 42.8–51.7 million high-quality paired-end reads were retained after processing (Table S3). Phred scores and other quality control parameters indicated that the resulting RNA-seq data were of sufficient quality for further analyses.

Ninety-five percent of total clean reads were successfully aligned to the avocado genome using HISAT2. DESeq2 analysis of mapped and counted reads identified 631 genes which were differentially expressed ( $p_{adj} < 0.05$ ) during asymptomatic ASBVd infection of avocado nursery trees. Of these DEGs, 398 were upregulated, while the remaining 233 were downregulated during infection (Fig. 1). A PCA plot generated from transformed data for these DEGs revealed that infected and uninfected samples formed two different clusters, though infected samples had more variation between them than the uninfected samples (Fig. 2). This indicates that, while viroid infection has some common effects on avocado gene expression (accounting for variance between clusters), it is likely that individual trees may have different responses to infection by ASBVd (accounting for variance within the infected cluster). DEGs ( $p_{adj} < 0.05$ ) were filtered further to include only those with  $|\log_2FC| \geq 0.58$ . Using this  $\log_2FC$  threshold, the total number of DEGs was reduced to 343, of which 190 were upregulated and 153 were downregulated (Table S4).

#### 3.3. Functional classification of differentially expressed genes

The DEGs found in this study had been previously annotated by the Avocado Genome Consortium (unpublished results), and therefore putative functions had already been assigned for most of the DEGs (310 out of 343). To investigate whether certain pathways and processes were specifically altered during ASBVd infection, DEGs were subjected to GO enrichment analysis. GOSep analysis of upregulated DEGs ( $p_{adj} < 0.05$ ) showed that 21 GO terms were significantly enriched at  $p < 0.05$  (Fig. 3). The types of enriched GO terms were rather evenly distributed, with six

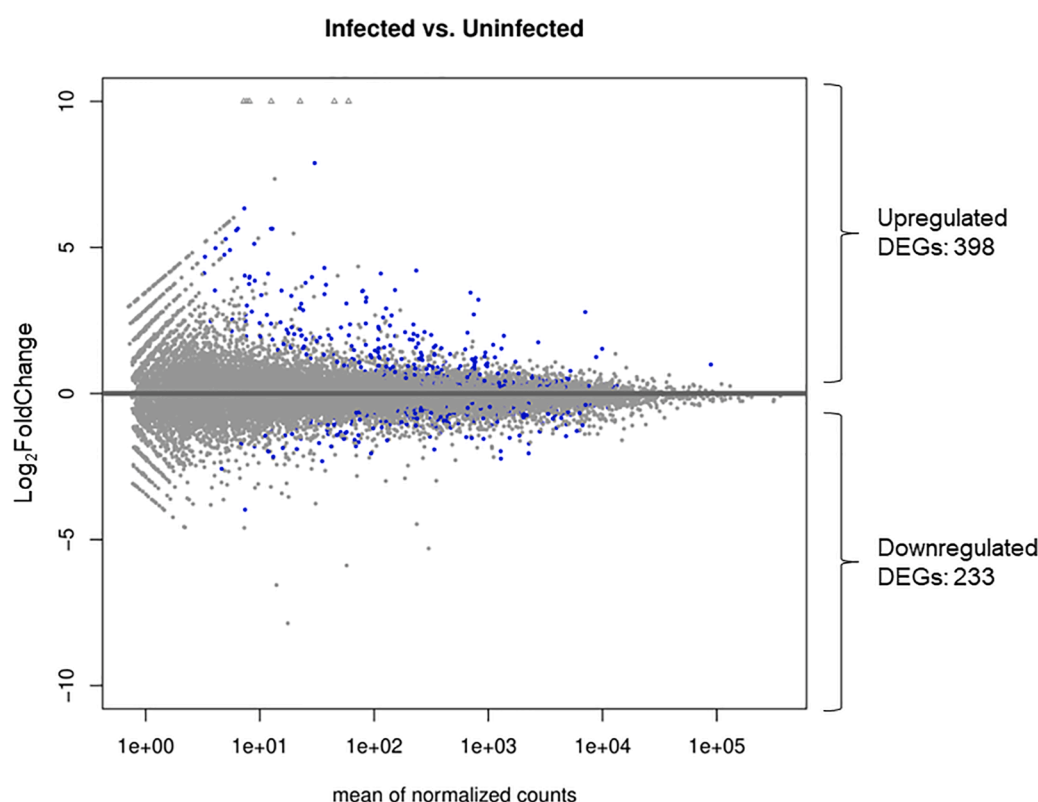


**Fig. 1.** Volcano plot of differentially expressed genes (DEGs) in asymptomatic ASBVd-infected avocado. Genes with a statistically significant  $\log_2$ FoldChange at  $p_{adj} < 0.05$  are indicated by blue dots on the volcano plot. Genes without significant differential expression are shown by grey dots.



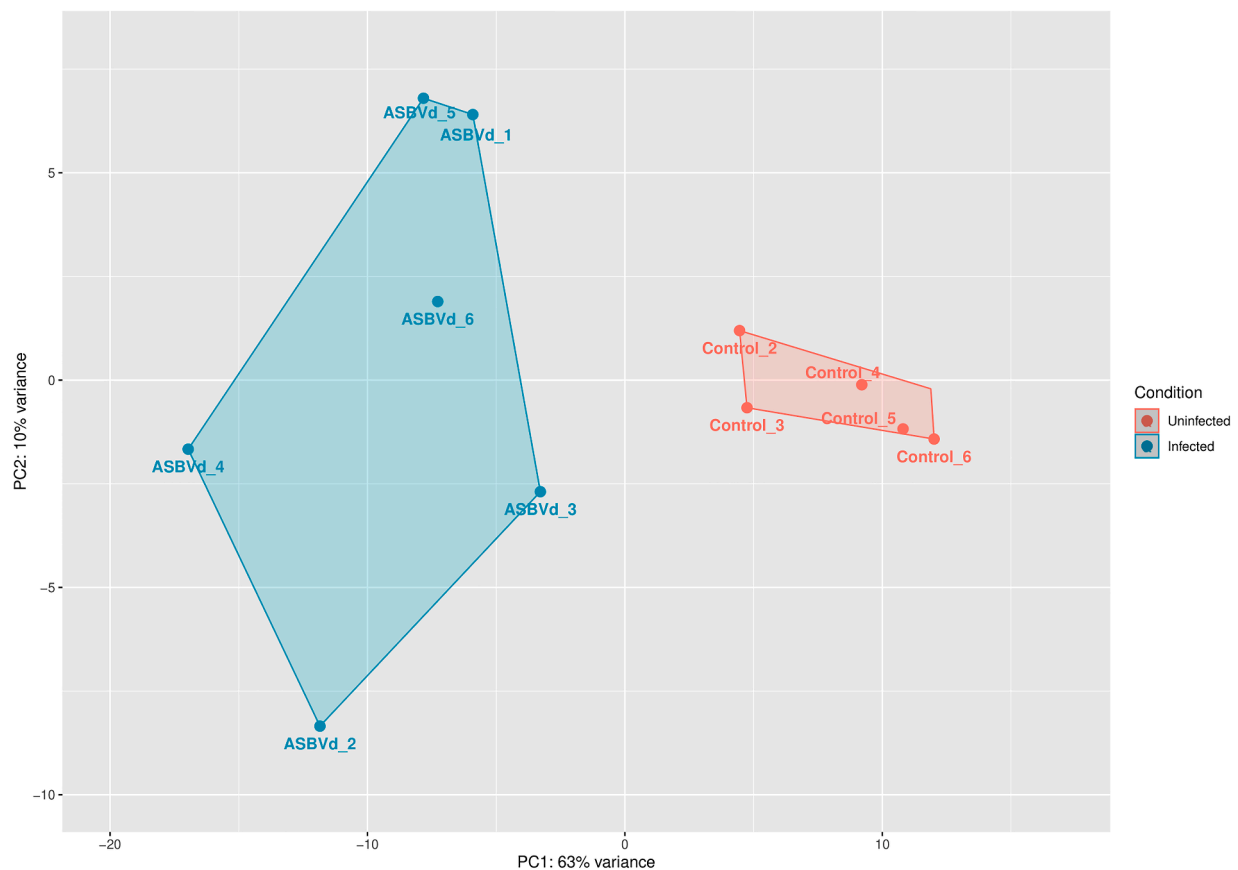


**Fig. 2.** Principal component analysis (PCA) plot of differentially expressed genes ( $p_{adj} < 0.05$ ) for uninfected and asymptomatic ASBVd-infected avocado samples, transformed using variance-stabilising transformation. Uninfected samples (turquoise dots) clustered closely together, while infected samples (red dots) exhibited more variation between biological replicates. The PCA plot shows distinct variance present between infected and uninfected groups.

terms enriched in the “biological process” category, eight terms in the “cellular component” category, and seven enriched terms in the “molecular function” category (Table S5). Interestingly, 14 of the 21 enriched GO terms were related to translation or processing of translation components in the cell. For the downregulated DEGs, however, no GO terms were significantly enriched at  $p < 0.05$  in this dataset.

To further categorise both up- and downregulated DEGs according to their functions in host pathways, MapMan was used to visualise expression of the 343 DEGs ( $p_{adj} < 0.05$ ;  $|\log_2FC| \geq 0.58$ ) according to the functional bins previously assigned by Mercator for this genome (Backer et al., 2022). MapMan analysis sorted 314 genes into respective bins, though several DEGs were assigned to multiple bins due to roles in different avocado pathways (see Table S6 for gene IDs and bin allocations). Redundant genes were subsequently removed, and an overview of specific cellular pathways was produced, revealing that 189 of the DEGs could be mapped to specific processes in the host cell (Fig. 4). The largest proportion of these genes (34 %) were mapped to biotic stress response pathways – shown as orange shapes in Fig. 4. Many DEGs were also attributed to functioning in gene expression processes such as transcription (30), translation (4), protein modification (13) and protein degradation (21). Genes functioning in secondary metabolism pathways were highly upregulated, with only 1 of 23 DEGs being suppressed (*C09g024100*,  $\log_2FC = -0.86$ ). Fifteen DEGs were mapped to hormone signalling networks (purple shapes in Fig. 4), with the majority (10 out of 15) being upregulated. Several genes encoding transporter proteins were also induced (11 out of 14) in asymptomatic ASBVd infection, while five genes related to cell wall synthesis, modification or degradation were differentially expressed in this interaction. MapMan visualisation thus showed that, although enriched GO terms were mainly limited to translation-related processes and components, several other

pathways and processes in avocado were extensively affected by ASBVd infection.

#### 3.4. ASBVd infection triggers host defence responses in asymptomatic avocado

Transcriptome analysis indicated that genes involved in pathogen-associated molecular pattern (PAMP)-triggered immunity (PTI) (basal defence response) and effector-triggered immunity (ETI) (a more vigorous defence response) were altered in their expression in ASBVd-infected avocado (Fig. 5a). Amongst the upregulated genes, which account for the majority of DEGs in the plant defence pathway, several *pathogenesis-related* (PR) genes were altered in their expression. One *PR-1* gene (*C10g019860*) was strongly induced ( $\log_2FC = 4.00$ ), along with two *chitinases* (*PR-3/PR-4*) (*C04g017400*;  $\log_2FC = 4.03$  and *C04g017350*;  $\log_2FC = 6.34$ ) and a *thaumatin-like protein* (*PR-5*) (*C06g018350*;  $\log_2FC = 4.75$ ). Nine genes encoding receptor-like kinases (RLKs), which, like PR proteins, play a role in basal immunity, were upregulated in ASBVd-infected plants (*C02g004610*, *C02g038880*, *C02g039020*, *C01g020430*, *C11g004120*, *C06g025450*, *C03g028110*, *C12g019160*, and *C03g029940*), while six RLKs were suppressed during infection (*C05g008940*, *C09g021400*, *C07g023540*, *C03g005060*, *C03g047860* and *C12g015400*) (Fig. 5b). Two WRKY transcription factors (TFs), which function in modifying expression of defence genes in plants, were upregulated in ASBVd-infected avocado — WRKY TF *C10g022730* was strongly induced, with a  $\log_2FC$  of 3.50.

Peroxidases, which play a role in biosynthesis of reactive oxygen species (ROS) during both PTI and ETI, were shown to be affected in their expression after ASBVd-infection. Four peroxidases were upregulated (*C04g027490*, *C06g009510*, *C02g053070*, and *C10g016550*) while

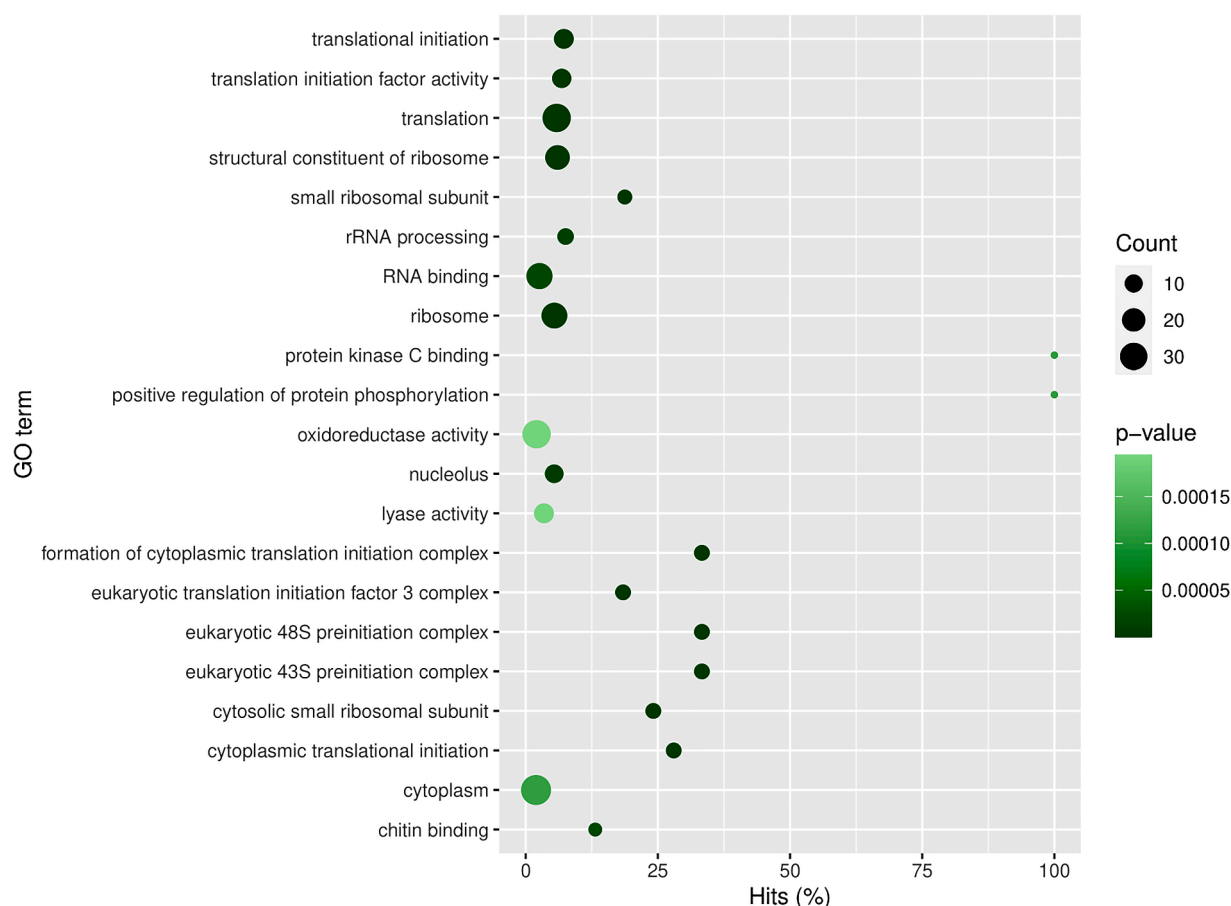


**Fig. 3.** Enriched gene ontology (GO) terms for differentially expressed genes (DEGs) ( $p_{adj} < 0.05$ ) which were upregulated during avocado sunblotch viroid (ASBVd) infection of avocado nursery trees. The number of DEGs in each category is represented as a percentage of total annotated avocado genes in that category (Hits%), shown along the x-axis. The over-represented  $p$ -value for each enriched GO term is indicated by the colour of the circles according to the corresponding legend.

one peroxidase was downregulated (C06g024460) (Figs. 4 and 5a). Three genes encoding the nucleotide-binding site leucine-rich repeat proteins (NBS-LRRs) — RGA2 (C10g007170 and C01g020090) and RPM1-like (C07g013030) — which form part of ETI in plants, were suppressed in infected avocado. Downregulated DEGs also included four components of calcium signalling pathways: one *calcium-dependant protein kinase (CDPK)* (C02g010990) and three *calcium-binding/calmodulin proteins (CaMs/CMLs)* (C03g035210, C01g016360 and C05g006980). Finally, some components of a non-specific host response to biotic stress, such as genes encoding heat shock proteins (HSPs) (C05g003020 and C06g004520) or wound-induced protein (WIN1) (C06g014700), were upregulated upon viroid infection (Fig. 5a).

### 3.5. Phytohormone signalling pathways are affected by ASBVd infection

Numerous genes relating to phytohormones — chemical messengers which influence several cellular pathways — had altered expression profiles in ASBVd-infected avocado (Fig. 5b). Five genes involved in cytokinin (CK) signalling, as identified by MapMan visualisation (Fig. 4), were all upregulated. The CK-related gene with the strongest increase in expression was the *CK dehydrogenase* C04g020150, which had a  $\log_2FC$  of 3.53. Three of the four *UDP-glycosyltransferases* that were assigned to the CK signalling bin by Mercator (C01g011340, C08g007610 and C11g017520) had BLAST hits with high similarity to a *7-deoxyloaaganetin glycosyltransferase-like* mRNA in *Magnolia sinica* — indicating these enzymes may instead function in secondary metabolism. Only one *UDP-glycosyltransferase* assigned to the CK bin (C10g014460) was similar to *zeatin O-xylosyltransferase (ZOX)*; an enzyme specific to CK signalling. Another upregulated *ZOX-like* gene (C02g037020) was sorted into the

abscisic acid (ABA)-related pathway, though this gene may function instead in the inactivation of CK.

An additional *UDP-glycosyltransferase* (C02g018760), assigned to the auxin pathway by MapMan due to its similarity to *Indole-3-acetate beta-glucosyltransferase (IAA-Glu synthetase)*, was upregulated in infected avocado. Two other auxin-related genes, *auxin response factor (ARF)* (C12g017050) and *auxin-responsive protein (SAUR71)* (C06g019430) were suppressed by viroid infection (Fig. 5b). It should be noted that the ARF shown in Fig. 5b (C12g017050) was not allocated to a functional bin by Mercator, but this DEG had 73 % BLAST similarity to *ARF 9-like* mRNA from *M. sinica*, confirming the putative annotation from the Peame105 genome.

The genes involved in ethylene (ET) signalling had varying expression profiles in ASBVd-infected avocado; the *Fe2OG dioxygenase domain-containing protein (2OGD)* (C05g025170), *1-aminocyclopropane-1-carboxylate (ACC) oxidase 1 (ACO1)* (C11g001540) and the ethylene-responsive TF *ERF113* (C03g031380) were upregulated. Three more *ERFs* (C04g025670, C01g018740 and C11g021440), an *ACC synthase (ACS)* (C06g005770), and the *universal stress protein A-like* (C07g029420) were downregulated in this interaction, with *ERF 109-like* (C04g025670) having the strongest suppression amongst phytohormone-related DEGs ( $\log_2FC = -3.98$ ). In the ABA pathway, a chloroplastic *9-cis-epoxycarotenoid dioxygenase (NECD)* (C06g015670) and a gene similar to *protein phosphatase 2C (PP2C)* (C09g015760) were downregulated during viroid infection (Fig. 5b), while the only DEG related to gibberellic acid (GA) signalling (C01g003640) had the second highest expression in the hormone signalling pathways ( $\log_2FC = 2.49$ ) (Fig. 4).

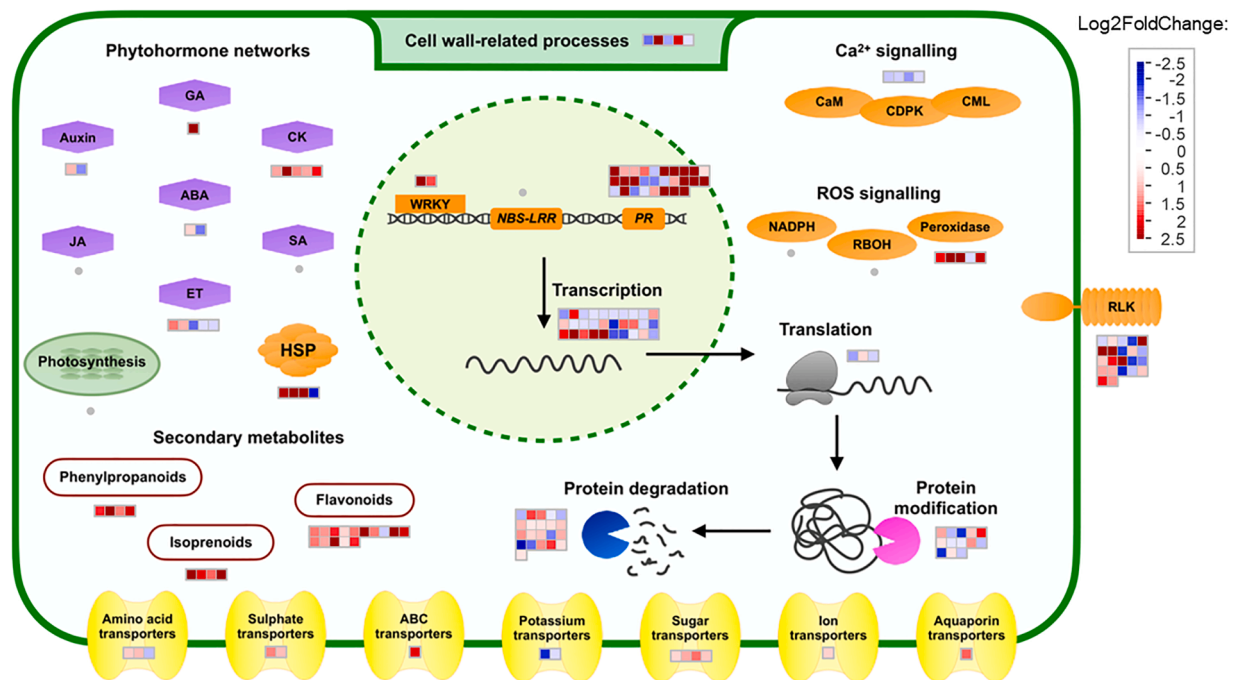


**Fig. 4.** MapMan visualisation of differential expression of genes in specific cellular pathways in asymptomatic ASBVd-infected avocado, using cut-off  $p_{adj} < 0.05$ ;  $|\log_2\text{FoldChange}| \geq 0.58$ . Changes in transcript abundance are shown as  $\log_2\text{FoldChange}$  relative to uninfected avocado (according to the scale provided) for each cellular component. Components belonging to networks with specific functions are colour-coded as follows: components of plant immunity are shown in orange; hormone signalling components are in purple; pathways in secondary metabolism are indicated by white boxes outlined in red; and transporters are displayed in yellow. Each coloured block corresponds to a single differentially expressed gene (DEG) linked to a particular pathway (individual gene identities shown in Table S6). Genes that are significantly downregulated during infection are indicated by blue blocks, while genes significantly upregulated during infection are shown by red blocks. Grey dots indicate that no DEGs were implicated in a particular pathway by Mercator-assigned bins. Abbreviations: ABA—abscisic acid; ABC—ATP-binding cassette; BR—brassinosteroid; CAM—calcium-binding calmodulin proteins; CDPK—calcium dependant protein kinase; CK—cytokinin; CML—calmodulin-like protein; ET—ethylene; GA—gibberellic acid; HSP—heat shock protein; JA—jasmonic acid; NBS-LRR—nucleotide-binding site leucine-rich repeat protein; PR—pathogenesis-related genes; RBOH—respiratory burst oxidase homologue; RLK—receptor-like kinase; ROS—reactive oxygen species; SA—salicylic acid.

### 3.6. Transcription factors are differentially expressed in ASBVd-infected avocado

Global changes in gene expression, such as those observed in viroid-infected avocado, may be linked to the differential accumulation of TFs inside host cells. MapMan analysis showed that 30 TF genes were differentially expressed after ASBVd infection (Fig. 4), and examination of gene annotations in the Peame105 genome identified three more DEGs that were downregulated. TFs with links to defence responses (WRKY TFs) and hormone signalling pathways (ERFs and ARFs) were shown in corresponding heatmaps for simpler visualisation (Fig. 5a & b) and have been discussed in the above sections. The remaining 25 TFs, most of which were downregulated in infected avocado, are visualised separately in Fig. 5c. The two TF genes with the highest upregulation, *TGA2* (C05g014460;  $\log_2\text{FC} = 5.58$ ) and *BZIP domain-containing protein* (C03g045670;  $\log_2\text{FC} = 2.41$ ), both belong to the basic leucine zipper (BZIP) family of TFs, though two other members of this TF family were downregulated (C06g006130 and C02g012200). Four members of the bHLH (basic-helix-loop-helix) TF family (C09g009650, C05g027690, C06g027730 and C02g020280) were all suppressed in this interaction, while MYB family TFs, which made up the most abundant of the TF families, were found amongst both the up- and downregulated DEGs (Fig. 5c).

### 3.7. RT-qPCR analysis validates RNA-seq expression data

RT-qPCR was used to assess the expression of nine selected DEGs; *EFM*, *MST3*, *BGL/PR-2*, *ACS*, *CML24*, *GRP*, *PDDA*, *TIFY* and *TM53*. As observed in RNA-seq results, all nine genes were found to be significantly differentially expressed ( $p < 0.05$ ) in infected samples compared

to uninfected controls. *EFM*, *MST3*, and *BGL/PR-2* were upregulated, while the remaining six genes were downregulated during infection. Comparison of  $\log_2\text{FC}$  of candidate DEGs in RT-qPCR and RNA-seq data revealed similar expression profiles in both data sets (Fig. 6).

## 4. Discussion

In this study, we produced the first global transcriptome of ASBVd-infected avocado. RNA-seq analysis revealed 631 DEGs (at  $p_{adj} < 0.05$ ), of which 343 had 1.5X higher or lower expression in infected samples ( $|\log_2\text{FC}| \geq 0.58$ ) — the highest number of DEGs found in an avsunviroid-infected host to date. Previously, a RT-qPCR study investigated the expression of four defence genes in leaves and fruit of mature avocado trees infected with ASBVd and found that only two of the genes were differentially expressed (López-Rivera et al., 2018). The only global transcriptome for a host infected with an avsunviroid published to date is a microarray analysis of asymptomatic peach infected with PLMVd (Herranz et al., 2013). The results of that investigation identified 16 DEGs in asymptomatic peach leaves, though authors speculated that some DEGs may have been missed due to the type of array used. Our data therefore represent a substantial contribution to the current knowledge of the response of plants to avsunviroid infection.

When compared to more recent RNA-seq analyses of hosts infected with pospiviroids, however, the 631 DEGs found in our study is relatively low. For example, 1530 DEGs ( $p < 0.05$ ;  $|\log_2\text{FC}| \geq 1.3$ ) were found in 'Etrog' citron (*Citrus medica*) infected with CEVd (Wang et al., 2019), while 1572 genes were differentially expressed in sweet cherry infected with HSVd (Xu et al., 2020) ( $p < 0.05$ ;  $|\log_2\text{FC}| \geq 2$ ). In tomato (*Solanum lycopersicum*) infected with a severe variant of PSTVd, researchers found 2731 DEGs ( $p < 0.05$ ;  $|\text{FC}| \geq 2$ ), while 933 DEGs were

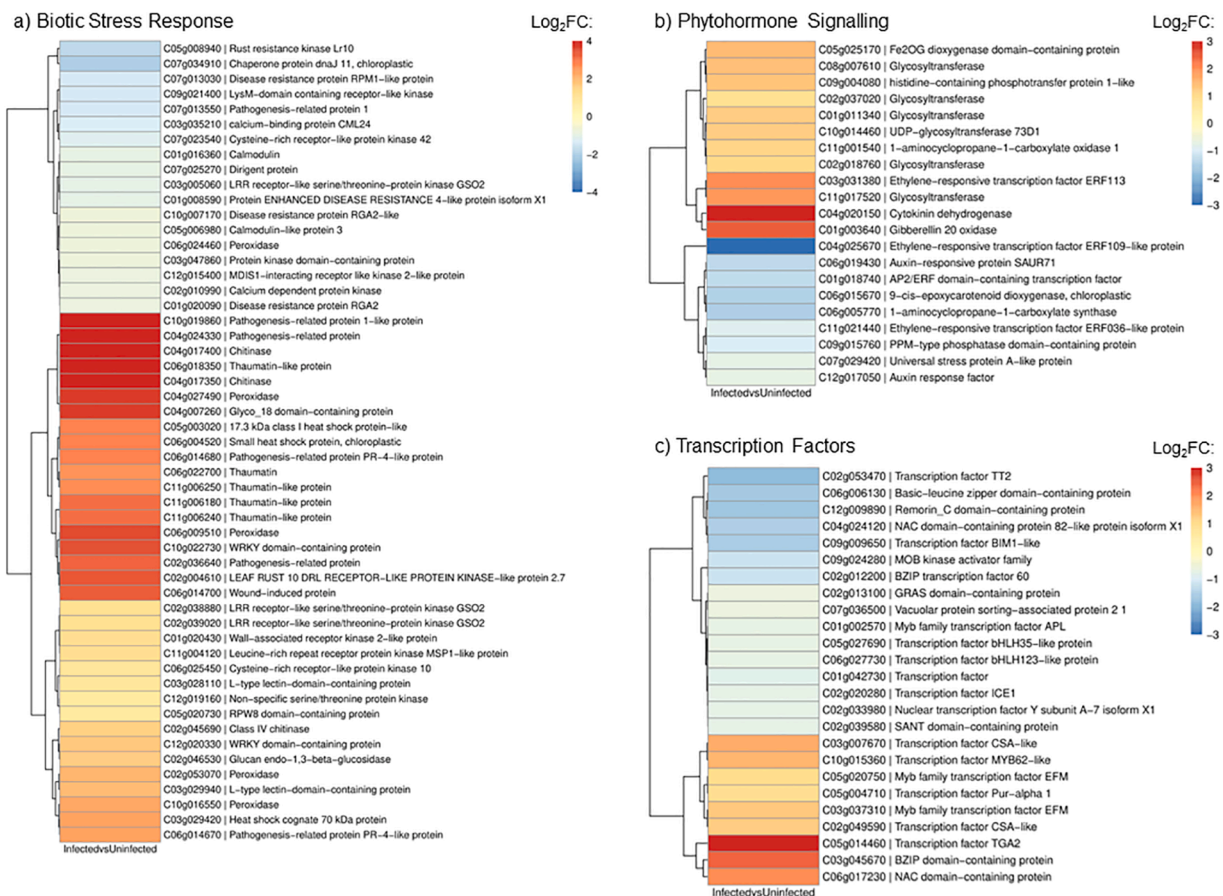


**Fig. 5.** Heat cluster maps of genes related to biotic stress response (a), phytohormone signalling (b) and transcription (c) which were significantly differentially expressed ( $p_{adj} < 0.05$ ;  $|\log_2\text{FoldChange}| \geq 0.58$ ) in avocado infected with avocado sunblotch viroid (ASBVd). Gene expression is indicated as Log<sub>2</sub>FoldChange (Log<sub>2</sub>FC) relative to uninfected controls, colour-coded according to the corresponding legends. Genes were functionally classified according to MapMan analysis and their putative annotations. Genes on the heat maps are named according to their identifiers in the *Persea americana* West Indian pure accession genome (Peame105), and putative annotations are shown.

identified in the same host species infected with a mild PSTVd variant. It is worth mentioning, however, that the high number of DEGs in those studies were found in symptomatic (not asymptomatic) interactions of hosts with pospiviroids (not avsunviroids).

The lower number of DEGs found in our study and PLMVd-infected peach (Herranz et al., 2013) compared to pospiviroid studies may be due to the asymptomatic nature of the interactions studied, since the lack of phenotypic changes observed in these host plants would coincide with the limited changes in host gene expression. This finding also supports the assertions made by Flores et al. (2020), who claimed that diseases induced by members of the *Pospiviroidae* and *Avsunviroidae* families are innately different, and that the systemic symptoms induced by pospiviroids cannot be directly compared with local symptoms observed in avsunviroid infections. Future investigations into global changes in gene expression induced by avsunviroid infection will reveal whether limited transcriptome changes are common to all host interactions with members of this viroid family.

Despite differences in diseases caused by pospiviroids and avsunviroids, the cellular pathways affected in ASBVd-infected avocado were comparable to those observed in other viroid-host interactions. One host pathway where DEGs were commonly observed in viroid-infected hosts was plant immune response (Joubert et al., 2022). In this study we observed the upregulation of 14 PR genes and several different RLKs in infected avocado, suggesting that PTI is induced by ASBVd; this result correlates with the findings of other viroid-host transcriptome studies, which showed that PR genes and RLKs are induced in PSTVd-infected tomato, CEVd-infected 'Etrog' citron, and in hop (*Humulus lupulus*)

infected with citrus bark-cracking viroid (CBCVd) (Mishra et al., 2018; Wang et al., 2019; Więsyk et al., 2018). In contrast to the findings in those studies, four calcium-signalling related genes were downregulated in ASBVd-infected avocado, and no MAP (mitogen-activated protein) kinases were differentially expressed in this interaction. Since MAP kinase- and calcium-signalling pathways have roles in activating components of both PTI and ETI (Lu and Tsuda, 2021), the lack of activation or the suppression of genes in these respective signalling pathways may, to some extent, offset the induction of other components of plant immunity in viroid-infected avocado.

Phytohormone signalling genes in avocado, which also play a role in host response to biotic stress, were affected by ASBVd infection (Figs. 4 and 5b). Interestingly, MapMan analysis (Fig. 4) indicated that no DEGs were specifically mapped to salicylic acid (SA) or jasmonic acid (JA) signalling networks, though these hormones are especially recognised for their roles in plant defence responses. Two copies of the SA marker gene *PR1* were, however, induced during ASBVd infection in this study, while one copy was suppressed (Fig. 5a) — these were assigned to the PR gene bin by MapMan rather than the SA signalling bin due to overlapping functions, and were analysed as part of the biotic stress response genes in this study. Another SA-related gene, *NPR1*, is a regulator of SA signalling, and was not significantly differentially expressed in our data. This coincides with the results of a previous RT-qPCR analysis in ASBVd-infected avocado, which showed that *NPR1* was not significantly altered in its expression in symptomatic or asymptomatic tissues (López-Rivera et al., 2018).

Though the JA pathway was not affected in ASBVd-infected avocado,



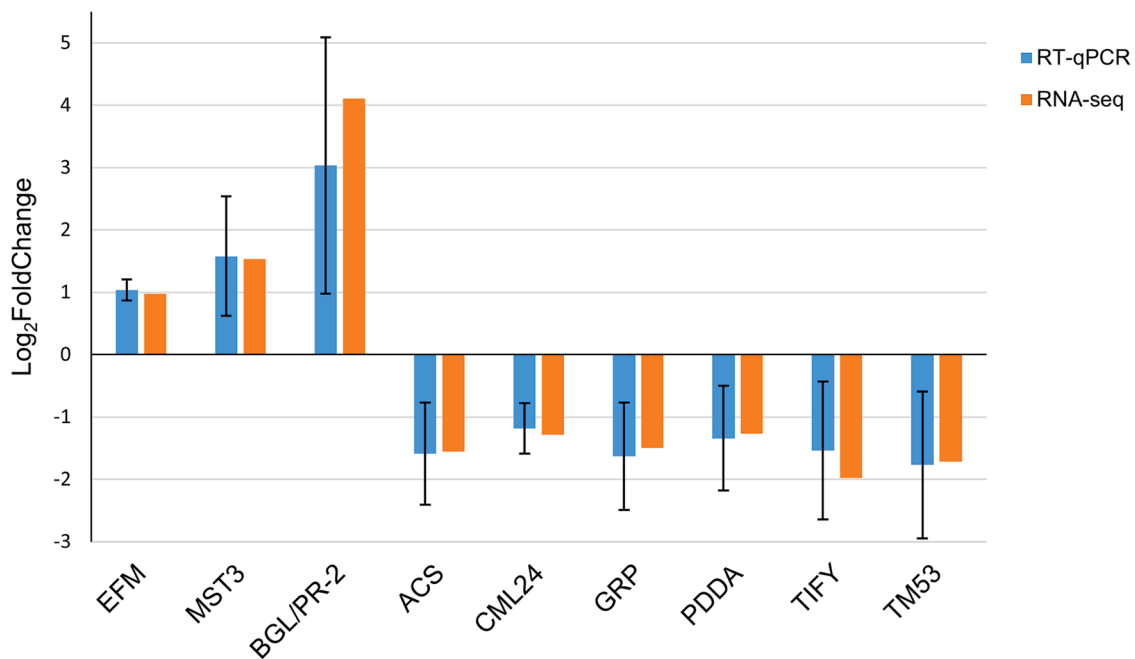


**Fig. 6.** Reverse transcriptase quantitative PCR (RT-qPCR) validation of randomly selected differentially expressed genes (DEGs) from RNA sequencing (RNA-seq) of avocado infected with avocado sunblotch viroid (ASBVd). Expression of each gene in infected samples is shown as Log<sub>2</sub>FoldChange relative to uninfected controls. In both RT-qPCR and RNA-seq data sets, all genes were significantly differentially expressed in infected samples (compared to uninfected samples) at  $p < 0.05$ . RT-qPCR data for each candidate DEG was normalised using *GAPDH* and *Polyubiquitin* as internal reference genes. Error bars represent standard deviation of means of six biological replicates. EFM, MYB family transcription factor EFM; MST3, Sugar transport protein MST3; BGL/PR-2, Glucan endo-1,3-beta-glucosidase (Pathogenesis-related protein 2); ACS, 1-aminocyclopropane-1-carboxylate synthase; CML24, Calcium-binding protein CML24; GRP, Glutaredoxin family protein; PDPA, Phospho-2-dehydro-3-deoxyheptonate aldolase; TIFY, Tify domain-containing protein; TM53, Transmembrane protein 53.

ethylene (ET) signalling, which acts synergistically to JA signalling, showed a few genes with differential expression (Figs. 4 and 5b). Genes involved in the ET pathway did not show trends in their overall expression during viroid infection, with two ET biosynthesis genes, *ACO1* and *ACS*, having opposite expression profiles in this interaction. Three out of four *ERFs* — TFs responsive to cellular ET levels — were induced upon ASBVd infection. Since these TFs are important regulators of plant stress responses (Xie et al., 2019), their increased expression may indicate that other host responses are activated downstream of these *ERFs* in response to altered ET levels.

Another hormone signalling network affected by ASBVd infection is that involving auxin. One *glycosyltransferase*, encoding a possible IAA-Glu synthetase, was induced in this interaction (*C02g018760*) (Fig. 5b). In contrast, two genes which encode auxin-response proteins SAUR71 (*C06g019430*) and ARF (*C12g017050*) were downregulated by viroid infection of avocado, similar to observations made for PSTVd-infected tomato (Więsyk et al., 2018). Auxins play a crucial role in plant growth, with functions in several cellular processes (Sauer et al., 2013). We postulate that altered auxin homeostasis during viroid infection may result in the “sprawling growth habit” that has been observed for both symptomatic and asymptomatic ASBVd-infected avocado trees (Kuhn et al., 2017). The modified gene expression shown here identifies a starting point for future experiments to investigate whether hormonal changes may be related to the altered growth habit of ASBVd-infected avocado.

Changes in expression of different cellular signalling components upon ASBVd infection may be due to the induction or suppression of certain TFs in this interaction. MapMan analysis showed 30 putative TFs that were altered in their expression (Fig. 4). Multiple TFs belonging to the WRKY, AP2/ERF, bZIP, bHLH, NAC and MYB families were identified (Fig. 5a, b & c). These TFs have been shown to regulate components of phytohormone networks, plant immunity, and plant response to stress (Ambawat et al., 2013; Dröge-Laser et al., 2018; Sun et al., 2018; Yuan et al., 2019) and were differentially expressed in several viroid-host

interactions studied to date (Joubert et al., 2022). We hypothesise that altered accumulation of TFs in ASBVd-infected avocado may be responsible for downstream effects on host gene expression observed in this study, though the initial mechanism influencing TF expression remains to be elucidated.

While the focus of our study was the differential transcription of specific genes, it cannot be disregarded that transcript accumulation may not correspond with the proteins produced from translation of those transcripts, since components involved in translation as well as protein degradation had altered expression during ASBVd infection (Figs. 3 and 4). Indeed, the upregulation of translation components could offset the suppression of other DEGs analysed in this study, if transcripts with reduced numbers are subject to increased protein synthesis in host cells. Similarly, DEGs induced upon viroid infection may not correspond to increased protein accumulation, since enhanced transcription may be countered by increased degradation of proteins downstream. This must be taken into account when considering any transcriptome studies, since RNA-seq data is insufficient to draw conclusions regarding the effect of viroid infection on host protein functioning.

The function of host proteins is also largely influenced by the phosphorylation state of these molecules, which is determined by protein kinases. Thirteen genes involved in post-translational modification of proteins were differentially expressed in ASBVd-infected avocado (Fig. 4). The altered accumulation of protein kinases in this interaction could have downstream effects on cellular signalling pathways, since changes in the phosphorylation status of other proteins in signalling cascades would modify the activity of affected proteins. The possible influence this would have on the functioning of proteins produced by all DEGs in this interaction must be considered when drawing conclusions from transcriptome data.

## 5. Conclusion

This study represents the first investigation into changes in global

gene expression induced by ASBVd, and the first RNA-seq analysis of a host infected with an avsunviroid. Transcriptome data revealed a relatively low number of DEGs in asymptomatic avocado nursery trees infected with ASBVd when compared to RNA-seq analyses in pospiviroid-infected hosts, though this may be due to the different nature of disease caused by the two viroid families. Future research should investigate global gene expression in ASBVd-infected avocado with chlorotic symptoms to determine whether the number of DEGs is substantially increased in the symptomatic interaction. Investigations into the transcriptome of other hosts infected with avsunviroids will further elucidate the differences between host responses to the two viroid families. Finally, these transcriptome data can be used as a basis for studies in the future, which can explore the metabolome and/or proteome of viroid-infected avocado to corroborate findings regarding the host response to ASBVd infection.

## Funding

This study was funded by the Hans Merensky Foundation and the Research Development Programme (RDP) of the University of Pretoria.

## CRediT authorship contribution statement

**M. Joubert:** Conceptualization, Data curation, Formal analysis, Investigation, Methodology, Visualization, Writing – original draft. **N. van den Berg:** Conceptualization, Funding acquisition, Supervision, Writing – review & editing. **J. Theron:** Supervision, Writing – review & editing. **V. Swart:** Conceptualization, Funding acquisition, Methodology, Supervision, Writing – review & editing.

## Declaration of Competing Interest

The authors declare that they have no known competing financial interests or personal relationships that could have appeared to influence the work reported in this paper.

## Data availability

Data has been made available as specified in the Materials and methods section of this article.

## Acknowledgements

The authors would like to thank all South African avocado nurseries that contributed plant material to this project. We are grateful to Dr Robert Backer for assistance with bioinformatic analyses and to Ms Alicia Fick for creative support. We also thank MacroGen Europe and the DNA Sanger Sequencing facility at the University of Pretoria for sequencing services.

## Supplementary materials

Supplementary material associated with this article can be found, in the online version, at [doi:10.1016/j.virusres.2023.199263](https://doi.org/10.1016/j.virusres.2023.199263).

## References

- Allen, R., Palukaitis, P., Symons, R., 1981. Purified avocado sunblotch viroid causes disease in avocado seedlings. *Australas. Plant Pathol.* 10 (2), 31–32.
- Ambawat, S., Sharma, P., Yadav, N.R., Yadav, R.C., 2013. MYB transcription factor genes as regulators for plant responses: an overview. *Physiol. Mol. Biol. Plants* 19 (3), 307–321.
- Andrews, S., 2010. FastQC: a quality control tool for high throughput sequence data.
- Backer, R., Engelbrecht, J., Van den Berg, N., 2022. Differing responses to *Phytophthora cinnamomi* infection in susceptible and partially resistant *Persea americana* (Mill.) rootstocks: a case for the role of receptor-like kinases and apoplastic proteases. *Front. Plant Sci.* 13, 928176.
- Bolger, A.M., Lohse, M., Usadel, B., 2014. Trimmomatic: a flexible trimmer for Illumina sequence data. *Bioinformatics* 30 (15), 2114–2120.
- Chang, S., Puryear, J., Cairney, J., 1993. A simple and efficient method for isolating RNA from pine trees. *Plant Mol. Biol. Rep.* 11 (2), 113–116.
- Chi, S., Zhang, J., Li, H., Wang, P., Feng, L., Ren, Y., 2022. RNA-seq profiling reveals the transcriptional response against potato spindle tuber viroid in different potato cultivars and developmental stages. *Potato Res.* 1–12.
- Delgado, S., Navarro, B., Serra, P., Gentile, P., Cambra, M.-Á., Chiumenti, M., De Stradis, A., Di Serio, F., Flores, R., 2019. How sequence variants of a plastid-replicating viroid with one single nucleotide change initiate disease in its natural host. *RNA Biol.* 16 (7), 906–917.
- Di Serio, F., Li, S.-F., Matoušek, J., Owens, R.A., Pallás, V., Randles, J.W., Sano, T., Verhoeven, J.T.J., Vidalakis, G., Flores, R., 2018. ICTV virus taxonomy profile: *avsunviroidae*. *J. Gen. Virol.* 99 (5), 611–612.
- Di Serio, F., Owens, R.A., Li, S.-F., Matoušek, J., Pallás, V., Randles, J.W., Sano, T., Verhoeven, J.T.J., Vidalakis, G., Flores, R., 2021. ICTV virus taxonomy profile: *pospiviroidae*. *J. Gen. Virol.* 102 (2), 001543.
- Dröge-Laser, W., Snoek, B.L., Snel, B., Weiste, C., 2018. The *Arabidopsis* bZIP transcription factor family—An update. *Curr. Opin. Plant Biol.* 45, 36–49.
- Engelbrecht, J., Duong, T.A., Van den Berg, N., 2013. Development of a nested quantitative real-time PCR for detecting *Phytophthora cinnamomi* in *Persea americana* rootstocks. *Plant Dis.* 97 (8), 1012–1017.
- Ewels, P., Magnusson, M., Lundin, S., Käller, M., 2016. MultiQC: summarize analysis results for multiple tools and samples in a single report. *Bioinformatics* 32 (19), 3047–3048.
- Flores, R., Gago-Zachert, S., Serra, P., De la Pena, M., Navarro, B., 2017a. Chrysanthemum chlorotic mottle viroid. In: Hadidi, A., Flores, R., Randles, J.W., Palukaitis, P. (Eds.), *Viroids and Satellites*. Academic Press, pp. 331–338.
- Flores, R., Navarro, B., Delgado, S., Hernández, C., Xu, W.-X., Barba, M., Hadidi, A., Di Serio, F., 2017b. Peach latent mosaic viroid in infected peach. In: Hadidi, A., Flores, R., Randles, J.W., Palukaitis, P. (Eds.), *Viroids and Satellites*. Academic Press, pp. 307–316.
- Flores, R., Navarro, B., Delgado, S., Serra, P., Di Serio, F., 2020. Viroid pathogenesis: a critical appraisal of the role of RNA silencing in triggering the initial molecular lesion. *FEMS Microbiol. Rev.* 44 (3), 386–398.
- Geering, A., Steele, V., Kopittke, R., 2006. Final Report For Horticulture Australia Limited Project AV03009: Development of Avocado Sunblotch Viroid Indexing Protocols for the Avocado Nursery Industry. University of Queensland.
- Góra-Sochacka, A., Wiśnyk, A., Fogtman, A., Lirski, M., Zagórski-Ostoja, W., 2019. Root transcriptomic analysis reveals global changes induced by systemic infection of *Solanum lycopersicum* with mild and severe variants of potato spindle tuber viroid. *Viruses* 11 (11), 992.
- Hadjieva, N., Apostolova, E., Baev, V., Yahubyan, G., Gozmanova, M., 2021. Transcriptome analysis reveals dynamic cultivar-dependent patterns of gene expression in potato spindle tuber viroid-infected pepper. *Plants* 10 (12), 2687.
- Herranz, M.C., Niehl, A., Rosales, M., Fiore, N., Zamorano, A., Granell, A., Pallas, V., 2013. A remarkable synergistic effect at the transcriptomic level in peach fruits doubly infected by *prunus necrotic ringspot virus* and *peach latent mosaic viroid*. *Virol. J.* 10, 164.
- Joubert, M., van den Berg, N., Theron, J., Swart, V., 2022. Transcriptomics advancement in the complex response of plants to viroid infection. *Int. J. Mol. Sci.* 23 (14), 7677.
- Kim, D., Langmead, B., Salzberg, S.L., 2015. HISAT: a fast spliced aligner with low memory requirements. *Nat. Methods* 12 (4), 357–360.
- Kolde, R., 2012. Pheatmap: pretty heatmaps. *R package version 1(2)*.
- Kuhn, D.N., Freeman, B., Geering, A., Chambers, A.H., 2019. A highly sensitive method to detect avocado sunblotch viroid for the maintenance of infection-free avocado germplasm collections. *Viruses* 11 (6), 512.
- Kuhn, D.N., Geering, A.D., Dixon, J., 2017. Avocado sunblotch viroid. In: Hadidi, A., Flores, R., Randles, J.W., Palukaitis, P. (Eds.), *Viroids and Satellites*. Academic Press, pp. 297–305.
- Lavagi-Craddock, I., Dang, T., Comstock, S., Osman, F., Bodaghi, S., Vidalakis, G., 2022. Transcriptome analysis of citrus dwarfing viroid induced dwarfing phenotype of sweet orange on trifoliate orange rootstock. *Microorganisms* 10 (6), 1144.
- Li, H., Handsaker, B., Wysoker, A., Fennell, T., Ruan, J., Homer, N., Marth, G., Abecasis, G., Durbin, R., Subgroup, G.P.D.P., 2009. The sequence alignment/map format and SAMtools. *Bioinformatics* 25 (16), 2078–2079.
- Li, S., Wu, Z.-G., Zhou, Y., Dong, Z.-F., Fei, X., Zhou, C.-Y., Li, S.-F., 2022. Changes in metabolism modulate induced by viroid infection in the orchid *Dendrobium officinale*. *Virus Res.* 308, 198626.
- Liao, Y., Smyth, G.K., Shi, W., 2014. featureCounts: an efficient general purpose program for assigning sequence reads to genomic features. *Bioinformatics* 30 (7), 923–930.
- Lohse, M., Nagel, A., Herter, T., May, P., Schroda, M., Zrenner, R., Tohge, T., Fernie, A.R., Stitt, M., Usadel, B., 2014. Mercator: a fast and simple web server for genome scale functional annotation of plant sequence data. *Plant Cell Environ.* 37 (12), 1250–1258.
- López-Rivera, L.A., Ramírez-Ramírez, I., González-Hernández, V.A., Cruz-Huerta, N., Téliz-Ortiz, D., 2018. Differential gene expression of avocado defense genes in response to avocado sunblotch viroid infection. *Rev. Mex. Fitopatol.* 36 (1), 151–161.
- Love, M.I., Huber, W., Anders, S., 2014. Moderated estimation of fold change and dispersion for RNA-seq data with DESeq2. *Genome Biol.* 15 (12), 550.
- Lu, Y., Tsuda, K., 2021. Intimate association of PRR- and NLR-mediated signaling in plant immunity. *Mol. Plant Microbe Interact.* 34 (1), 3–14.
- Mishra, A.K., Kumar, A., Mishra, D., Nath, V.S., Jakše, J., Kocábek, T., Killi, U.K., Morina, F., Matoušek, J., 2018. Genome-wide transcriptomic analysis reveals insights into the response to *citrus bark cracking viroid* (CBCVd) in hop (*Humulus lupulus* L.). *Viruses* 10 (10), 570.

- Morey-León, G., Ortega-Ramirez, E., Julca-Chunga, C., Santos-Chanta, C., Graterol-Caldera, L., Mialhe, E., 2018. The detection of avocado sunblotch viroid in avocado using a real-time reverse transcriptase polymerase chain reaction. *BioTechnologia* 99 (2), 99–107.
- Navarro, B., Gisel, A., Rodio, M.E., Delgado, S., Flores, R., Di Serio, F., 2012. Small RNAs containing the pathogenic determinant of a chloroplast-replicating viroid guide the degradation of a host mRNA as predicted by RNA silencing. *Plant J.* 70 (6), 991–1003.
- Palukaitis, P., Hatta, T., Alexander, D.M., Symons, R.H., 1979. Characterization of a viroid associated with avocado sunblotch disease. *Virology* 99 (1), 145–151.
- Posit Team, 2022. RStudio: Integrated Development Environment For R. Posit Software, PBC, Boston, MA.
- Sauer, M., Robert, S., Kleine-Vehn, J., 2013. Auxin: simply complicated. *J. Exp. Bot.* 64 (9), 2565–2577.
- Schnell, R., Kuhn, D., Olano, C., Quintanilla, W., 2001a. Sequence diversity among avocado sunblotch viroids isolated from single avocado trees. *Phytoparasitica* 29 (5), 451–460.
- Schnell, R.J., Olano, C.T., Kuhn, D.N., 2001b. Detection of avocado sunblotch viroid variants using fluorescent single-strand conformation polymorphism analysis. *Electrophoresis* 22 (3), 427–432.
- Schwacke, R., Ponce-Soto, G.Y., Krause, K., Bolger, A.M., Arsova, B., Hallab, A., Gruden, K., Stitt, M., Bolger, M.E., Usadel, B., 2019. MapMan4: a refined protein classification and annotation framework applicable to multi-omics data analysis. *Mol. Plant* 12 (6), 879–892.
- Semancik, J., Szychowski, J., 1994. Avocado sunblotch disease: a persistent viroid infection in which variants are associated with differential symptoms. *J. Gen. Virol.* 75 (7), 1543–1549.
- Serra, P., Navarro, B., Forment, J., Gisel, A., Gago-Zachert, S., Di Serio, F., Flores, R., 2023. Expression of symptoms elicited by a hammerhead viroid through RNA silencing is related to population bottlenecks in the infected host. *New Phytol.* 239, 240–254.
- Sun, X., Wang, Y., Sui, N., 2018. Transcriptional regulation of bHLH during plant response to stress. *Biochem. Biophys. Res. Commun.* 503 (2), 397–401.
- Symons, R.H., 1981. Avocado sunblotch viroid: primary sequence and proposed secondary structure. *Nucleic Acids. Res.* 9 (23), 6527–6537.
- Wang, Y., Wu, J., Qiu, Y., Atta, S., Zhou, C., Cao, M., 2019. Global transcriptomic analysis reveals insights into the response of 'Etrog' citron (*Citrus medica* L.) to *Citrus Exocortis* Viroid infection. *Viruses* 11 (5), 453.
- Więsyk, A., Iwanicka-Nowicka, R., Fogtman, A., Zagórski-Ostoja, W., Góra-Sochacka, A., 2018. Time-course microarray analysis reveals differences between transcriptional changes in tomato leaves triggered by mild and severe variants of potato spindle tuber viroid. *Viruses* 10 (5), 257.
- Więsyk, A., Lirski, M., Fogtman, A., Zagórski-Ostoja, W., Góra-Sochacka, A., 2020. Differences in gene expression profiles at the early stage of *Solanum lycopersicum* infection with mild and severe variants of potato spindle tuber viroid. *Virus Res.* 286, 198090.
- Xia, C., Li, S., Hou, W., Fan, Z., Xiao, H., Lu, M., Sano, T., Zhang, Z., 2017. Global transcriptomic changes induced by infection of cucumber (*Cucumis sativus* L.) with mild and severe variants of *hop stunt viroid*. *Front. Microbiol.* 8, 2427.
- Xie, Z., Nolan, T.M., Jiang, H., Yin, Y., 2019. AP2/ERF transcription factor regulatory networks in hormone and abiotic stress responses in *Arabidopsis*. *Front. Plant Sci.* 10 (228).
- Xu, L., Zong, X., Wang, J., Wei, H., Chen, X., Liu, Q., 2020. Transcriptomic analysis reveals insights into the response to *Hop stunt viroid* (HSVd) in sweet cherry (*Prunus avium* L.) fruits. *PeerJ* 8, e10005.
- Young, M.D., Wakefield, M.J., Smyth, G.K., Oshlack, A., 2010. Gene ontology analysis for RNA-seq: accounting for selection bias. *Genome Biol.* 11 (2), 1–12.
- Yuan, X., Wang, H., Cai, J., Li, D., Song, F., 2019. NAC transcription factors in plant immunity. *Phytopathol. Res.* 1 (1), 1–13.